The impact of the self-interaction error on the density functional theory description of dissociating radical cations: Ionic and covalent dissociation limits

Jürgen Gräfenstein, Elfi Kraka, and Dieter Cremer
Department of Theoretical Chemistry, Göteborg University, Box 460, SE-403 50 Göteborg, Sweden

(Received 2 September 2003; accepted 8 October 2003)

Self-interaction corrected density functional theory was used to determine the self-interaction error for dissociating one-electron bonds. The self-interaction error of the unpaired electron mimics nondynamic correlation effects that have no physical basis where these effects increase for increasing separation distance. For short distances the magnitude of the self-interaction error takes a minimum and increases then again for decreasing *R*. The position of the minimum of the magnitude of the self-interaction error influences the equilibrium properties of the one-electron bond in the radical cations H_2^+ (**1**), $B_2H_4^+$ (**2**), and $C_2H_6^+$ (**3**), which differ significantly. These differences are explained by hyperconjugative interactions in **2** and **3** that are directly reflected by the self-interaction error and its orbital contributions. The density functional theory description of the dissociating radical cations suffers not only from the self-interaction error but also from the simplified description of interelectronic exchange. The calculated differences between ionic and covalent dissociation for **1**, **2**, and **3** provide an excellent criterion for determining the basic failures of density functional theory, self-interaction corrected density functional theory, and other methods. Pure electronic, orbital relaxation, and geometric relaxation contributions to the self-interaction error are discussed. The relevance of these effects for the description of transition states and charge transfer complexes is shown. Suggestions for the construction of new exchange-correlation functionals are given. In this connection, the disadvantages of recently suggested self-interaction error-free density functional theory methods are emphasized. © *2004 American Institute of Physics.* [DOI: 10.1063/1.1630017]

I. INTRODUCTION

In recent work,[1–7] we have derived a number of tools to investigate the self-interaction error (SIE) of standard Kohn–Sham density functional theory (KS-DFT) (Refs. 8 and 9) when carried out with the approximate functionals available today.[10–40] The SIE of DFT exchange (SIE-X) mimics long-range correlation effects, which are responsible for (a) the stability of restricted KS solutions and (b) help to describe electron systems with considerable multireference character.[1–7] This can be shown by calculating the changes in the one-electron density distribution caused by the SIE (Refs. 1–3) or alternatively investigating the structure of the exchange hole at typical positions in a molecule [e.g., at the centroids of the localized molecular orbitals (LMOs) occupied by core, bond, and lone pair electrons].[4–6] By splitting the exchange hole into a self-interaction corrected (SIC) part and a SIE part, into a self-exchange (intraelectronic) and an interelectronic part or into orbital contributions, the implications of the SIE for the description of electron correlation as it is accounted for by approximate exchange functionals can be demonstrated.[4–6]

First studies on the SIE of DFT reach back to early work by Fermi and Amaldi.[29] The problems the SIE might cause were already anticipated by Slater,[30] however a first detailed discussion of the SIE was given by Perdew and Zunger in 1981.[11] These authors introduced an orbital-dependent SIC formalism, which is the basis of most SIE-free DFT investigations published until now. (For reviews on SIC-DFT, see Refs. 1, 10, and 27.)

The SIE-X is a direct consequence of the localized character of the DFT exchange hole. It compensates for the difference between the delocalized SIC-DFT hole, which resembles the exact exchange hole, and the local DFT exchange hole. This leads to the advantage of adding (in an unspecified way) important long-range correlation effects, however leads also to serious drawbacks in the case of odd electron systems:[31–40] The dissociation of one and three-electron bonds is wrongly described. Reaction barriers involving an odd number of electrons are underestimated. Bonding and electron distribution in charge transfer complexes can be wrongly predicted.[32] In this work, we will concentrate on the dissociation of one-electron bonds in radical cations and show that, although these systems have been already investigated by several authors,[26(c),31,33–40] there are still a number of open questions, which are essential for the understanding of bonding in these molecules in specific and the performance of DFT in general.

The dissociation of an odd-electron bond proceeds in an asymmetric fashion, i.e., the unpaired electron moves to one of the fragments so that a radical and a cation (one-electron bonds) or a closed shell fragment and a radical cation (three-electron bonds) are generated. For one-electron bonds this phenomenon is known as charge-spin separation: for large

distances R between the fragments, the positive charge is concentrated at the ionic fragment and the spin density at the radicalic one. (For three-electron bonds, charge and spin become concentrated at the same fragment.) This charge-spin separation has led several authors[33,38] to the conclusion that a correct quantum-chemical description of odd-electron-bond breaking has to predict an ionic ground state (i.e., one ionic and one neutral fragment) rather than a covalent one (i.e., two fragments with charge $+1/2$ each) in the limit of a large distance between the fragments. This means that at a certain interaction distance the covalent ground state should become electronically unstable and bifurcate into two equivalent ionic ones.

Hartree–Fock (HF) calculations provide such a bifurcation, and it has been concluded that HF allows for a qualitatively correct description of dissociating radical cations.[38] Correlated wave-function methods tend to stabilize the covalent state relative to the ionic one and reduce the charge and spin separation for a given interfragment distance. DFT calculations, in distinction to HF, predict a covalent ground state for all interfragment distances with a drastically reduced limit energy for large bond lengths.[31,33,36–39] The ionic DFT state provides the correct limit energy for large interfragment distances. However, this state is electronically unstable, which has been called ''inverse symmetry breaking'' in the literature.[33]

Chermette and co-workers[38] pointed out that the DFT dissociation curves for diatomic molecules may jump back and forth between the covalent and the ionic state for moderate bond lengths (2–3 Å). This was interpreted as a fingerprint of an avoided crossing between the bonding covalent state and the ionic state. The authors argued that the bonding Σ_g and the antibonding Σ_u state belong to the same irreducible representation, viz. Σ, with respect to the $C_{\infty v}$ symmetry of the ionic states, which allows for an interaction between these states and makes an avoided crossing possible. Furthermore, the authors suggested that the occurrence of two equivalent, and thus degenerate, ionic states may give rise to nondynamic correlation effects in the dissociating radical cation and that the qualitatively incorrect DFT description of radical cations may be ascribed to the general limitations of DFT in describing nondynamic correlations.

The energy balance between the ionic and the covalent state is of crucial importance for an accurate description of odd-electron bond breaking. In the current paper, we will therefore discuss this energy balance in detail for dissociating one-electron-bonded radical cations and give an interpretation for the different descriptions one obtains at different levels of theory with the focus on DFT methods. We will calculate the SIE and its orbital contributions in dependence of the separation distance and we will show the following:

(1) HF, DFT, and in general methods without a specific type of nondynamic electron correlation fail to describe dissociation of one-electron bonds correctly. We will introduce criteria that provide a quantitative ordering of the performance of different methods.
(2) We will show that SIC-DFT is the method with the best performance, however we will also demonstrate that this is the result of a serious artifact of DFT, which was so far overlooked: DFT suffers also from an oversimplified description of interelectronic exchange that together with the SIE causes problems when describing the dissociation of radical cations.
(3) We will further discuss the influence of geometry relaxation on radical cation dissociation. Depending on the fact whether the fragments become Jahn-Teller unstable, geometry relaxation is particularly strong and changes the ideal dissociation behavior of the radical cation.
(4) The magnitude of the SIE increases not only for an increase in the separation distance R, but below a critical R value also for a decrease of R. The critical R value can be predicted from the electronic structure of the radical cation. It decides on the properties of the equilibrium geometry calculated by DFT or SIC-DFT.

Although our discussion will focus just on the prototypic radical cations H_2^+ (**1**), $B_2H_4^+$ (**2**), and $C_2H_6^+$ (**3**), the observations made will be of direct consequence for the description of reactions involving an odd number of electrons. Furthermore, we will be able to draw conclusions on the best way of curing DFT from the SIE.

The results obtained in this work will be presented in the following way: In Sec. II, the basic theory of the SIE and the SIC-DFT method used in this work are shortly described. Details of the computations are given in Sec. III. In Sec. IV, the SIE of radical cations is decomposed in pure electronic, orbital relaxation, and geometry relaxation effects. Investigation of its dependence on R supported by the analysis of the exchange hole at different R values leads to a clear insight into the performance of DFT in odd electron cases. Ionic and covalent dissociation limits of radical cations are also discussed in Sec. IV and their relevance for different methods are shown. Finally, in Sec. V the conclusions of this work, especially with regard to the application of DFT in odd electron cases are drawn.

II. BASIC THEORY OF THE SIE AND THE SIC-DFT METHOD

In a one-electron system, the exchange energy E_X exactly cancels the Coulomb energy J of the one electron, and the correlation energy E_C vanishes. Hence, for any α-spin density ϱ_α that integrates to one, the following relations must hold:

$$E_X[\varrho_\alpha,0]=-J[\varrho_\alpha], \tag{1a}$$

$$E_C[\varrho_\alpha,0]=0. \tag{1b}$$

The available approximate XC functionals violate one or both of conditions (1a), (1b) and contain thus a physically incorrect self-interaction of the electrons. Perdew and Zunger (PZ) (Ref. 11) suggested to start from one of the available approximate XC functionals and to augment it by a SIC term that cancels the self interaction orbital by orbital. The PZ SIC-XC functional takes the form

$$E_{XC}^{\text{correct}}=E_{XC}^{\text{approx}}[\varrho_\alpha,\varrho_\beta]-E_{XC}^{\text{SIE}}, \tag{2a}$$

$$E_{XC}^{\text{SIE}}=E_X^{\text{SIE}}+E_C^{\text{SIE}}, \tag{2b}$$

$$E_X^{\mathrm{SIE}} = \sum_{\sigma=\alpha,\beta} \sum_{i=1}^{N_\sigma} (E_X[\varrho_{i\sigma},0] + J[\varrho_{i\sigma}]), \tag{2c}$$

$$E_C^{\mathrm{SIE}} = \sum_{\sigma=\alpha,\beta} \sum_{i=1}^{N_\sigma} E_C[\varrho_{i\sigma},0], \tag{2d}$$

where $\varrho_{i\sigma}(\mathbf{r}) = |\varphi_{i\sigma}(\mathbf{r})|^2$ is the density that corresponds to the KS spin orbital $\varphi_{i\sigma}$.

The inclusion of the SIC terms into the XC functional alters the KS equations in two ways: First, the KS operator $\hat{F}$ is augmented by an additional orbital-dependent term,

$$\hat{F}_i^{\mathrm{SIC}}(\mathbf{r}) = \hat{F} - \hat{F}_i^{\mathrm{SIE}}, \tag{3a}$$

$$\hat{F}_i^{\mathrm{SIE}} = \int \mathrm{d}^3 r' \frac{\varrho_i(\mathbf{r}')}{|\mathbf{r}-\mathbf{r}'|} + \hat{V}_{\mathrm{XC}}[\varrho_i,0]. \tag{3b}$$

(We suppress the explicit spin indices here and in the following.) Second, contrary to the standard KS XC energy functional, $E_{\mathrm{XC}}^{\mathrm{SIE}}$ is no longer invariant with respect to rotations among the occupied orbitals. In addition to the usual KS conditions

$$\langle \varphi_a | \hat{F}_i^{\mathrm{SIE}} | \varphi_i \rangle = 0, \tag{4a}$$

the KS orbitals in SIC-DFT have to obey Eq. (4b) (see e.g., Ref. 17):

$$\langle \varphi_j | \hat{F}_i^{\mathrm{SIE}} - \hat{F}_j^{\mathrm{SIE}} | \varphi_i \rangle = 0 \tag{4b}$$

(indices *i*, *j* denote occupied, indices *a*, *b* virtual orbitals). Equation (4b) implies that in SIC-DFT there is no longer any freedom to represent the occupied KS orbitals in either canonical or localized form; instead, this choice is stipulated by the energy minimization. As a rule, the optimal KS orbitals turn out to be localized.[13]

Solving Eqs. (4a) and (4b) self-consistently is difficult and time-consuming. A reasonable compromise in many cases is to perform a standard KS-DFT calculation and to calculate $E_{\mathrm{XC}}^{\mathrm{SIE}}$ subsequently. KS-DFT gives no clue as to how the orbitals should be chosen to maximize $E_{\mathrm{XC}}^{\mathrm{SIE}}$ (and hence minimize the total energy). In self-consistent (SC) SIC-DFT calculations, the optimal KS orbitals are localized in most cases, and therefore $E_{\mathrm{XC}}^{\mathrm{SIE}}$ is usually calculated from localized molecular orbitals (LMOs). The resulting perturbative (P-) SIC-DFT makes it possible to estimate the pure electronic effects of the SIE and SIC-DFT at relatively low computational cost compared to a standard DFT calculation.

Both P-SIC-DFT and SC-SIC-DFT have been implemented in the COLOGNE 2003 program package.[41] P-SIC-DFT was implemented into an existing SCF code of COLOGNE 2003, which uses repeated diagonalization of the Fock matrix. The orbital localization is done according to the Foster–Boys[42] criterion. For the implementation of SC-SIC-DFT, a repeated diagonalization of the Fock matrix is an inappropriate approach because, due to Eq. (4b), the occupied orbitals are not invariant with respect to internal rotations and, in addition, localized, i.e., essentially different from the canonical orbitals generated in standard KS-DFT calculations. Therefore, the SC-SIC-DFT equations are solved with a univariate search method similar to that of Seeger and Pople.[43] Both a scaled steepest-descent approach and a conjugate-gradient approach[44] were programmed and implemented in COLOGNE 2003.[41] Test calculations showed that the conjugate-gradient approach reduced the number of necessary iterations in a SC-SIC-DFT calculations by up to a factor of 5.

III. COMPUTATIONAL DETAILS

Dissociation energies D_e, equilibrium bond distances r_e, harmonic vibration frequencies ω_e, and dissociation curves were calculated for H_2^+ (**1**), $B_2H_4^+$ (**2**), and $C_2H_6^+$ (**3**), which are typical representatives for a large class of molecules with one-electron bonds. Values D_e and the dissociation curves were calculated relative to the energies of the fragments (i.e., not relative to a supermolecule): $D_e = E(X_2^+) - E(X^\bullet) - E(X^+)$. The calculations were done at different levels of theories. A series of standard-KS calculations was performed to investigate the impact of the SIE for pure and hybrid DFT methods. We combined the Lee–Yang–Parr (LYP) correlation functional[45] with different mixtures of Becke 88 (Ref. 46) and exact HF exchange increasing the latter by the factor a_{HF}: pure Becke 88 (B) exchange ($a_{\mathrm{HF}}=0$), Becke 3 (B3) exchange[47] ($a_{\mathrm{HF}}=0.2$), Becke half-and-half exchange[48] ($a_{\mathrm{HF}}=0.5$), and pure HF exchange ($a_{\mathrm{HF}}=1$). It should be noted that we used the standard B3LYP functional, in which 19% of the LYP correlation energy are replaced by the Vosko–Wilk–Nusair (VWN) functional (the functional referred to as functional III in Ref. 49).

In addition to the standard DFT calculations, P-SIC-BLYP and SC-SIC-BLYP calculations were carried out using the direct minimization procedure described in the previous section. Finally, as a reference, we calculated equilibrium bond distances, dissociation energies, and binding curves for **2** and **3** at the CCSD(T) level of theory.[50] When calculating the dissociation curves of **2** and **3**, the distance *R* between the heavy atoms was used as reaction coordinate and the geometry of the molecule was reoptimized for each *R* considered. For the SC-SIC-DFT calculations, the corresponding CCSD(T) geometries were used, otherwise all geometries were optimized with the current method. Dunning's valence triple-zeta basis set cc-pVTZ (Ref. 51) was used for all calculations except the SC-SIC calculations where we had to resort to Dunning's valence double-zeta basis set cc-pVDZ (Ref. 51) to avoid convergence problems.

For P-SIC, SC-SIC, and CCSD(T), analytical energy gradients were not available. Therefore, the quantities r_e and D_e were determined by interpolating the calculated points on the dissociation curve with a cubic spline and calculating the minimum of this spline function. As for the impact of the SIE on the vibrational spectrum, we evaluated the adiabatic stretching frequencies ω_e^a(X–X) (Ref. 52) (X=H,B,C) for **1**, **2**, and **3** at all levels of theory used. The force constant belonging to the adiabatic stretching frequency is the curvature of the dissociation curve at r_e. For **1**, the adiabatic vibrational mode is identical with the harmonic vibration. In this case, a comparison of the calculated values of the ω_e^a and ω_e provides an insight into the numerical error brought about by the spline interpolation.

For the purpose of investigating the existence and stabil-

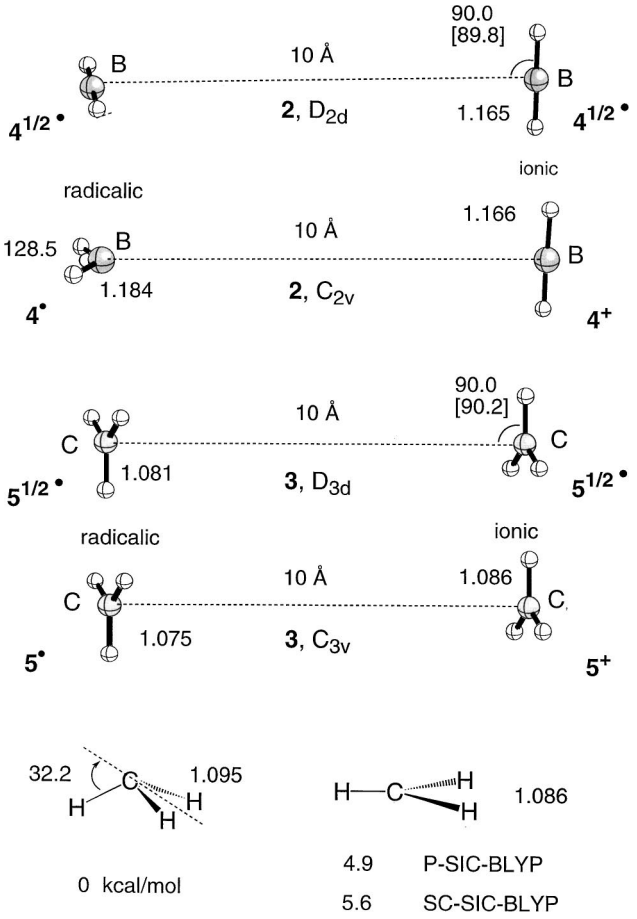

FIG. 1. BLYP/cc-pVTZ geometries used for the stability investigations of the covalent and ionic states of $B_2H_4^+$ and $C_2H_6^+$. Values in square brackets refer to the CCSD(T)/cc-pVTZ geometries (see Sec. III for details). Bond lengths in Å, angles in deg.

ity of covalent and ionic states, each of these states was calculated for **1**, **2**, and **3** at a bond length of 10 Å with the four DFT functionals mentioned above, additionally with HF and SC-SIC-BLYP. For **3**, the two states were calculated with Slater (S) exchange (Ref. 53) and the functional VWN5 of Vosko, Wilk, and Nusair[49] and SC-SIC-SVWN5 in addition. Stability tests[54,55] were performed for all methods except SC-SIC. In a first approach, CCSD(T)/cc-pVTZ-based geometries were used in all SC-SIC calculations. These geometries were prepared in the following ways: For the ionic states, we started from the geometries of the neutral and ionic fragments, i.e., BH_2 ($\mathbf{4}^{\bullet}$) and BH_2^+ ($\mathbf{4}^+$) for **2**, CH_3 ($\mathbf{5}^{\bullet}$) and CH_3^+ ($\mathbf{5}^+$) for **3**, and assembled these fragments at a distance of 10 Å between the heavy atoms using the appropriate symmetry (C_{2v} according to HBBH dihedral angles of 90° for **2**, C_{3v} in the staggered conformation for **3**). For the covalent states, we performed CCSD(T)/cc-pVTZ geometry optimizations. The fragments in the covalent states were forced to be planar, i.e., we adjusted the CCH and BBH bond angles to exactly 90° to make the geometries consistent to those of the ionic states. The CCSD(T) geometries were tested by numerical SC-SIC-DFT optimizations, which led to some unexpected results. CCSD(T) and SC-SIC-BLYP geometries are shown in Fig. 1. While SIC-DFT calculations were done with COLOGNE 2003 (Ref. 41) using the method described above, ACES 2 (Ref. 56) was used for the CCSD(T) calculations, and GAUSSIAN 98 (Ref. 57) for all other calculations.

IV. RESULTS AND DISCUSSION

Table I presents heavy atom dissociation energies, equilibrium distances, and vibrational frequencies for **1**, **2**, and **3**. In Table II, the SIE calculated for the radical cations is partitioned into a pure electronic, an orbital relaxation, and a geometry relaxation part using P-SIC and SC-SIC energies for BLYP at fixed and optimized geometries.

A. Investigation of the self-interaction error

For the three radical cations, DFT overbinds the molecular cations by 4–5 kcal/mol. The overbinding decreases as the portion of exact exchange in the XC functional is increased. HFLYP, which exclusively contains exact exchange,

TABLE I. Dissociation energies, equilibrium bond lengths, and harmonic vibrational frequencies for radical cations **1**, **2**, and **3**.[a]

	1				**2**				**3**			
	D_e	r_e	ω_e	ω_e^a	D_e	r_e	ω_e	ω_e^a	D_e	r_e	ω_e	ω_e^a
BLYP	69.09	1.136	1881.8	1844	62.44	1.789	519.9	526	56.41	2.007	372.8	338
B3LYP	67.84	1.114	2003.6	1946	60.91	1.807	507.8	483	54.83	1.967	418.9	398
BH-HLYP	66.38	1.089	2140.1	2066	57.56	1.846	487.8	464	51.14	1.940	464.5	420
HFLYP	64.29	1.057	2335.8	2187	55.40	1.876	493.8	486	47.94	1.893	536.1	534
P-SIC-BLYP	64.36	1.046		2226	50.4	1.944		476	53.9	1.918		519
SC-SIC-BLYP	64.29	1.057		2187	54.6	1.922		535	56.5	1.944		564
CCSD(T)[b]	64.28	1.057		2187	58.24	1.830		523	52.48	1.931		520
Expt.[c]	64.42	1.052	2321									

[a]P-SIC-BLYP calculations at BLYP geometries, SC-SIC-BLYP calculations at CCSD(T) geometries. SC-SIC calculations done with Dunning's cc-pVDZ basis set (Ref. 51). All other calculations with Dunning's cc-pVTZ basis set (Ref. 51). Energies in kcal/mol, bond distances in Å, frequencies in cm^{-1}. The ω_e values shown are for the H–H, B–B, and C–C stretching vibrations, respectively. For an explanation of the adiabatic frequencies ω_e^a, see text and Ref. 52.

[b]For **1**, the UHF values are taken.

[c]From K. P. Huber and G. Herzberg, *Constants of Diatomic Molecules* (Van Nostrand Reinhold, New York, 1979). The D_e value has been calculated from the experimental D_0 and ω values.

TABLE II. Decomposition of the self-interaction error (SIE) on the dissociation energies of the hydrogen radical cation ion (**1**), the borane radical cation (**2**), and the ethane radical cation (**3**).[a]

Molecule	Method	Effect	SIE molecule	SIE fragments	ΔD_e	D_e
1	BLYP					69.10
	P-SIC	pe	3.86	−1.05	−4.91	64.18
	SC-SIC	or	−1.01	−0.36	0.10	64.28
	exact					64.42
2	BLYP					62.44
	P-SIC	pe	6.69	−5.68	−12.37	50.07
				(−5.68,0.25)		
	P-SIC, opt	gr	−1.80	−1.47	−0.33	50.40
	SC-SIC	or	−13.36	−9.89	3.47	53.54
				(4.99,−4.90)		
	SC-SIC, opt	gr	−1.32	−0.26	−1.06	54.60
	exact					58.24
3	BLYP					56.41
	P-SIC	pe	60.97	57.51	−3.46	52.95
				(18.63,38.88)		
	P-SIC, opt	gr	−1.45	−0.5	−0.95	53.90
	SC-SIC	or	−42.04	38.74	3.30	56.25
				(20.14,−18.60)		
	SC-SIC, opt	gr	−1.25	−1.0	−0.25	56.5
	exact					52.48

[a]All values in kcal/mol. Abbreviations denote the pure electronic (pe) effect, the orbital relaxation (or) effect, and the geometry relaxation (gr) effect of the SIE. ΔD_e gives the total SIE of molecule and fragments on the dissociation energy D_e. Exact D_e values are taken from the experimental value for **1** and the CCSD (T) values for **2** and **3** (see Table I). Numbers in parentheses denote the SIE for the ionic and radicalic fragment.

underestimates the binding energies of **2** and **3** by 3.1 and 4.5 kcal/mol, respectively [with reference to the CCSD(T) values, see Table I]. The inclusion of SIC counteracts the overbinding. P-SIC-BLYP reduces D_e values by 4.9 (**1**), 12.4 (**2**), and 3.5 kcal/mol (**3**) where the absolute effects on the radical cation are considerably larger but are partially compensated by the SIEs of the fragments. The adjustment of the orbitals to the self-interaction corrected description is significant for polyatomic radical cations: In the case of **2** the D_e value is increased again by 3.8 kcal/mol (thus compensating the P-SIC effect on D_e by almost 30%) whereas in the case of **3** the pure electronic effect is literally canceled by orbital relaxation. Geometry relaxation leads only to small changes both at the P-SIC and SC-SIC levels of theory (Table II).

In summary, SIC-DFT improves only the dissociation energy of **1** because SC-SIC-BLYP is identical with HF for a one-electron system such as **1**. SIC-DFT leads to no improvement in the case of radical cation **3** and even deteriorates the D_e value in the case of **2**. BLYP overestimates for **1** and **3** the bond lengths (1.136 and 2.007 Å, Table I) by nearly 0.1 Å [CCSD(T) values: 1.057 and 1.931 Å], whereas the BLYP bond length for **2** (1.789 Å) is too short by 0.04 Å [CCSD(T): 1.830 Å]. Increasing the portion of exact exchange will decrease the bond length in **1** and **3** but increase it in **2**: HFLYP (1.876 Å) gives too long a bond in **2** and too short one in **3** (1.893 Å). P-SIC, in contrast, predicts too short bonds in **1** (1.046 Å) and **3** (1.918 Å) and too long a bond in **2** (1.944 Å, Table I). SC-SIC shows the same trends, however, the deviations of the r_e values (1.057, 1.922, 1.944 Å) from the reference values are smaller than for P-SIC.

The vibrational frequencies follow the trends in the calculated bond lengths in the way that an underestimation of r_e leads to exaggeration, an overestimation to a reduction of the stretching frequency. The behavior of **2** is again opposite to that of **1** and **3**: For **1** and **3**, the frequencies increase, for **2** they decrease with increasing factor a_{HF}. Comparing ω_e and ω_e^a for the standard-DFT calculations for **2** and **3** one finds that the ω_e^a values correctly reflect trends in the vibrational frequencies. A caveat is however appropriate: The ω_e and ω_e^a values for **1** (which should be identical) differ by 60–150 cm^{-1} due to numerical errors in the spline-interpolation procedure used to calculate ω_e^a, which has to be considered when discussing the adiabatic stretching frequencies.

SIC-DFT fails to lead to a significant improvement in both D_e, r_e, or ω_e^a values of radical cations (with more than one electron). It seems to approach the HFLYP or BH-HLYP values. However this does not guarantee an improvement in the description of the equilibrium properties of the radical cations.

1. Analysis of the SIE in dependence of the separation distance

Figures 2(a), 2(b), and 2(c) show the dissociation curves for **1**, **2**, and **3** in the range 1.4–5 Å. All methods give a qualitatively correct description around the equilibrium bond distance, with the tendency of DFT to overbind the molecular cation. However, the DFT binding curves are qualitatively incorrect in the dissociation limit, as has been pointed out earlier.[31,33,38] Instead of increasing monotonously towards the limit of zero, the molecule passes an artificial transition state, and for larger interaction distances R the bond energy decreases and converges slowly towards a limit, which may even be below the bond energy at equilibrium. This incorrect

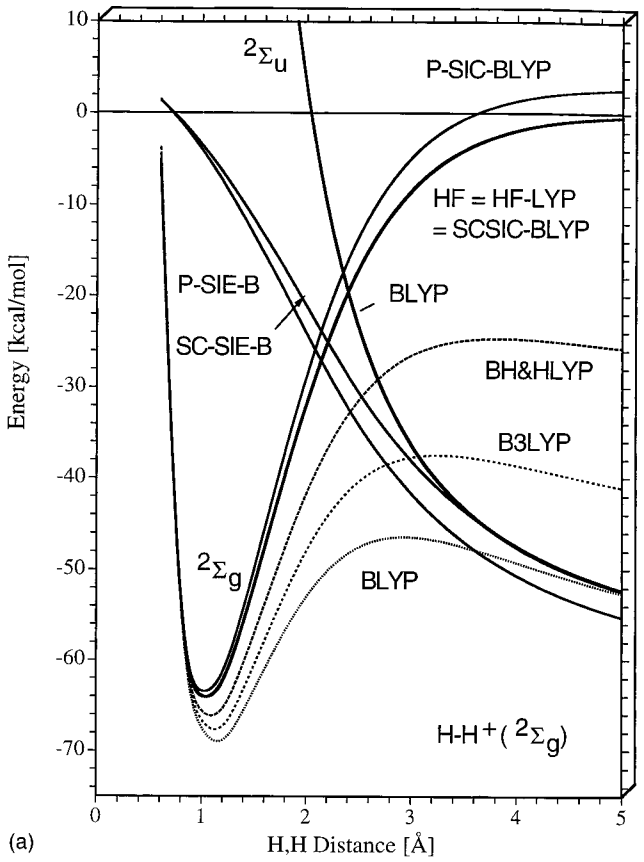

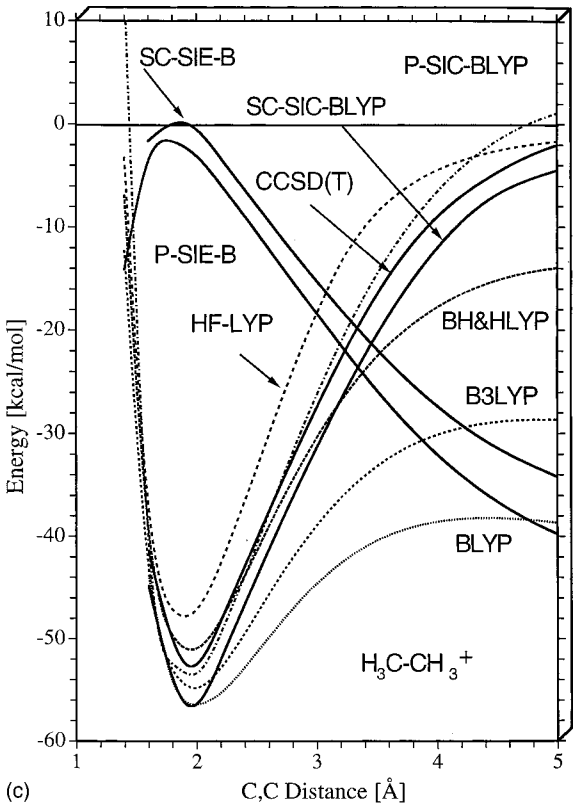

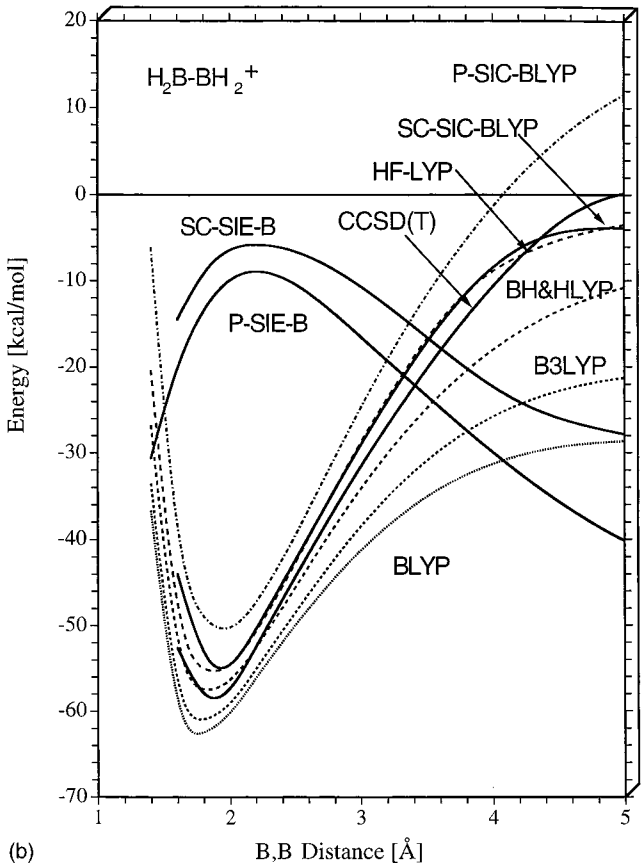

FIG. 2. Dissociation curves for H_2^+ (a), $B_2H_4^+$ (b), and $C_2H_6^+$ (c) calculated with DFT and wave-function methods. The SIE obtained with P-SIC-BLYP (P-SIE-B) and SC-SIC-BLYP (SC-SIE-B) is given relative to the SIEs of the fragments. Dunning's cc-pVTZ basis set (Ref. 51) was used for all calculations. For details of the calculations, see text.

behavior is present for all pure and hybrid DFT exchange functionals but becomes less distinct as a_{HF} increases. The transition state can be seen most clearly for **1** [Fig. 2(a)] but is also present for **2** and **3**, where it occurs at larger interaction distances.

HFLYP as well as SC-SIC-BLYP give a qualitatively correct description of the dissociation. P-SIC-BLYP overcompensates the error of BLYP, i.e., the supermolecule has a higher energy than the fragments for large interaction distances (Fig. 2). However, the absolute energy difference between supermolecule and fragments is smaller in the limit of large R for P-SIC-BLYP than for standard BLYP. The P-SIC energies are calculated based on a BLYP description, which predicts a covalent ground state even for large R, hence, supermolecule and fragments are described differently, which accounts for the energy difference. For SC-SIC, in contrast, one finds that the ground state becomes ionic beyond a certain R [defining a bifurcation point, at which a broken symmetry (BS) solution describing an ionic supermolecule state is lower in energy] for the two systems investigated. This means that supermolecule and fragment are described equivalently and thus have the same energy.

The fact that (i) the error in the description of the dissociation becomes smaller as a_{HF} increases and (ii) SC-SIC-DFT remedies the error indicate that the deviation should be caused by the SIE. The behavior of the SIE for large bond lengths R between the fragments A and B can be rationalized with a simple estimation.[12,36] Let ϱ_{A}^{v} and ϱ_{B}^{v} be the valence densities for the case that the unpaired electron is localized at A or B, respectively. The valence density of the covalent state is then to a good approximation $\varrho_{\mathrm{cov}}^{v}=(\varrho_{\mathrm{A}}^{v}+\varrho_{\mathrm{B}}^{v})/2$. The Coulomb self-interaction of the valence orbital for the ionic state is

$$J_{\mathrm{A}}=J_{\mathrm{B}}=\frac{1}{2}\int \mathrm{d}^3r_1\int \mathrm{d}^3r_2\frac{1}{r_{12}}\varrho_{\mathrm{A}}^{v}(\mathbf{r}_1)\varrho_{\mathrm{A}}^{v}(\mathbf{r}_2), \tag{5}$$

where $r_{12}=|\mathbf{r}_1-\mathbf{r}_2|$. For the covalent state, one will get

$$J_{\mathrm{cov}}=\frac{1}{2}J_A+\frac{1}{4R} \tag{6}$$

if one assumes that R is large compared to the spatial extent of ϱ_{A}^{v} and ϱ_{B}^{v}. The Coulomb self-interaction of the valence orbital behaves differently for the ionic and covalent states: While J_{A} is asymptotically constant, J_{cov} contains a term decaying as $1/4R$ resulting in an artificial Coulomb repulsion between the two halves of the valence charge.

The pure-DFT self-exchange energies for the two states are

$$E_{\mathrm{A}}^{\mathrm{X}}=E^{\mathrm{X}}[\varrho_{\mathrm{A}}^{v}], \tag{7a}$$

$$E_{\mathrm{cov}}^{\mathrm{X}}=2E^{\mathrm{X}}[\tfrac{1}{2}\varrho_{\mathrm{A}}^{v}] \tag{7b}$$

$$=CE_{\mathrm{A}}^{\mathrm{X}}. \tag{7c}$$

For LDA, $C=2^{-1/3}\approx 0.79$; for a gradient-corrected functional, C should be close to this value, hence, $C>1/2$ is to be expected in all cases. As has been suggested Noodleman and co-workers[54] and confirmed by Polo and co-workers,[4,5] the SIE is smaller in magnitude for a localized than a delocalized orbital, in particular if a GGA functional is used. In the ionic state, all orbitals are localized, hence one can expect that the magnitude of the SIE is small, i.e., $J_{\mathrm{A}}^{\mathrm{DFT}}\approx J_{\mathrm{A}}$. This assumption gives

$$E_{\mathrm{cov}}^{\mathrm{SIE}}\approx\underbrace{\left(\frac{1}{2}-C\right)}_{<0}J_A+\frac{1}{4R}. \tag{8}$$

Hence, for large R the SIE of the delocalized valence orbital, which makes the main contribution to the total SIE, contains a negative constant term, which accounts for the underbinding of radical cations in standard DFT, and a positive Coulomb term, which accounts for the repulsion of the fragments and the occurrence of an artificial transition state in the dissociation curve. In Fig. 2, both the calculated P-SIE-B and SC-SIE-B values are given as a function of R. Both curves are in agreement with Eq. (8) for large R. The SC-SIE-B curve approaches for all radical cations the BLYP dissociation curve and defines the limit for large R, which is equal to the self-repulsion J_A of one electron multiplied by the negative factor (0.5−C). The P-SIE-B curve is below the SC-SIE-B (the magnitude of the P-SIE contribution to D_e is always larger than that of the SC-SIE-B contribution) because of the missing orbital relaxation, which becomes larger for increasing R. If a hybrid functional is used expression (8) has to be multiplied by $1-a_{\mathrm{HF}}$, i.e., the qualitative behavior of the binding curve remains unchanged but the SIE and the corresponding error in the D_e values become smaller.

2. Exchange hole description of the SIE

In Fig. 3, the exchange hole of the single electron in **1** is shown for two R values as calculated with HF and two DFT functionals. Exchange is equal to self-exchange (intraelectronic exchange) in this case and the HF exchange hole corresponds to the negative density distribution of the single electron. The HF hole is delocalized and independent of the position of the electron, i.e., it is a static hole. The LDA hole shown in Fig. 3(a) (calculated with Slater exchange and using the HF density to facilitate the comparison) is localized at the position of the electron (in Fig. 3, this is the position of nucleus H1), spherically symmetric, and at its lowest point $-\rho(\mathbf{r})$. For a single electron the SIC-LDA hole is exactly equal to the HF exchange hole (provided the same density is used to describe the holes).

The difference between the LDA and the SIC-LDA hole defines the SIE part of the hole, which is also shown in Fig. 3(a). It describes a long-range correlation effect: If the single electron is positioned at H1 a second electron is most likely found at nucleus H2 thus separating two electrons by the internuclear distance [1 Å in Fig. 3(a)]. Hence, a nondynamic correlation effect is described by the LDA exchange hole, which is not needed in the case of a single electron so that an artificial stabilization results for the radical cation. It is this stabilization, which lowers the DFT energy of the radical cation and makes the covalent solution artificially stable against any symmetry breaking leading to the ionic solution.

In Fig. 3(b), the GGA exchange hole calculated for the PW91 exchange functional (for Becke 88 exchange an ex-

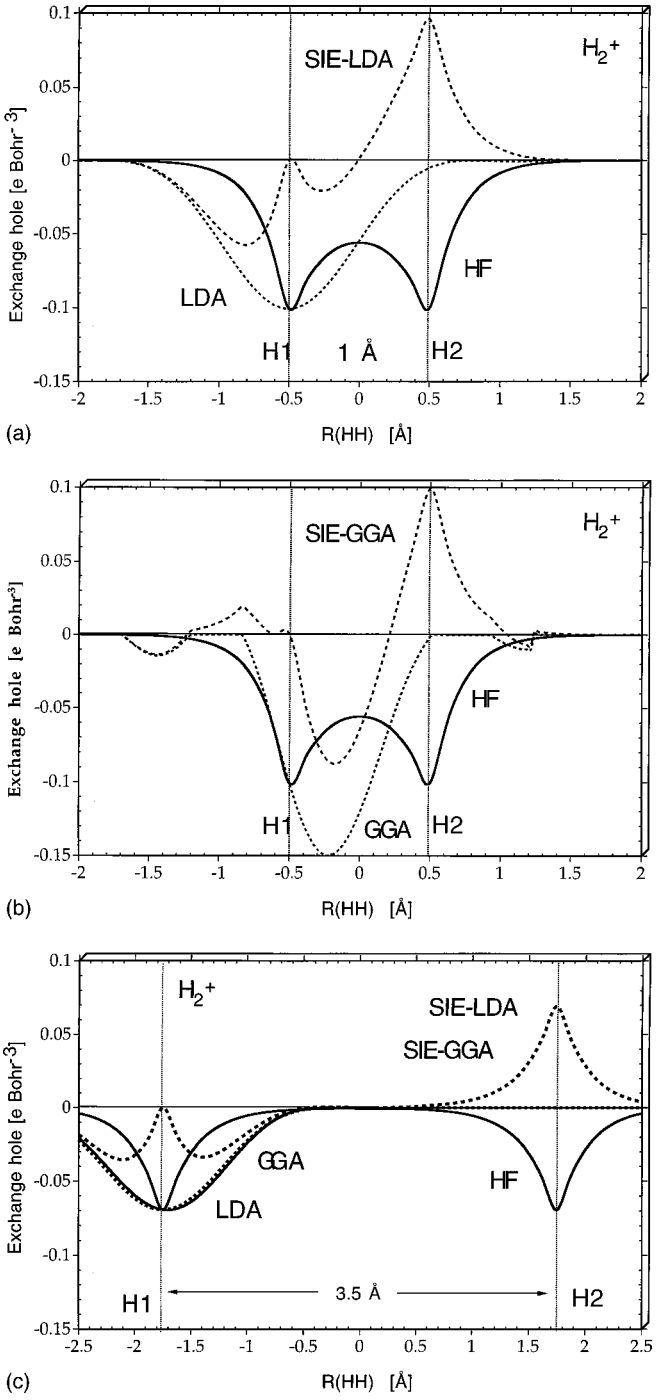

FIG. 3. Graphical representation of the exchange hole calculated for H_2^+ ($^2\Sigma_g$) along the bond axis at the HF, LDA (SVWN5), and GGA (PW91PW91) level of theory for separation distances of 1 (a) and 5 Å (c). The reference electron is positioned at H1. For one electron the HF exchange hole is equal to the SIC-DFT exchange hole. The SIE part of the DFT exchange hole is given as the difference between DFT and SIC-DFT exchange hole. All calculations with a cc-pVTZ basis set at the experimental geometry.

change hole is not defined) is shown. Although details of the exchange hole are now different compared to the LDA exchange hole (for a detailed discussion of the differences, see Ref. 5), the general conclusion with regard to the SIE hole remain the same: It describes a nondynamic correlation effect as if a second electron would be present.

At 3.5 Å, the HF exchange hole of the covalent state of **1** is delocalized over the whole internuclear separation distance [Fig. 3(c)]. The LDA and the GGA holes become identical because the densities of the two atoms resemble those of isolated atoms, which give for LDA and GGA the same exchange hole provided the reference electron is located at the nucleus where the reduced gradient vanishes. The SIE describes now an even stronger long range correlation effect (the virtual second electron is separated over a larger distance R), which leads to stronger stabilization. The form of the SIE hole converges to a limit that can be anticipated from the form of the SIE hole at 3.5 Å and this limit is given in Eq. (8) for $R\rightarrow\infty$ as $(0.5-C)J_A$. Since J_A is the self-repulsion part, which at the HF level is equal to the negative self-exchange part, the SIE hole at $R=\infty$ must be the negative of the HF exchange hole (provided the same density is used for the construction of the exchange holes). This means that the DFT dissociation curves in Fig. 2 converge to $(1-a_{\mathrm{HF}})(0.5-C)J_{\mathrm{A}}$.

3. The SIE at short separation distances

Exchange and SIE hole at $R=1$ Å [Figs. 3(a) and 3(b)] reveal that one can no longer speak of two separated negative charges of $0.5e$. Equations (5)–(8) hold for R values that are large enough so that the two fragments are well separated. For small R values, the atomic densities penetrate each other, a substantial bond density is present, and the SIE behaves differently than for large R. This is reflected most clearly by the SIE curves in Figs. 2(a), 2(b), and 2(c) in the R-range close to the equilibrium distance where $E_{\mathrm{cov}}^{\mathrm{SIE}}$ becomes less positive than predicted by Eq. (8). This implies a less negative derivative $\mathrm{d}E_{\mathrm{cov}}^{\mathrm{SIE}}/\mathrm{d}R$ than given by $-1/(4R^2)$ [see Eq. (8)]. The derivative $\mathrm{d}E_{\mathrm{cov}}^{\mathrm{SIE}}/\mathrm{d}R$ becomes even zero and then adopts positive values so that a maximum is found at $R\approx 2.2$ Å for **2** and at about 1.8 Å for **3**.

The deviations of $E_{\mathrm{cov}}^{\mathrm{SIE}}$ from the expression in Eq. (8) observed for small R have two reasons. Figure 4(a) gives the total SIE energy for **2** and its orbital contributions calculated at the P-SIC-BLYP level of theory. One sees that the SIE of the bond orbital determines largely the trend observed for the total P-SIE in Fig. 2(b). For small R, the spatial extent of $\varrho_{\mathrm{A,B}}^{v}$ plays an increasing role for the SIE of the valence electron as anticipated from the form of the exchange holes shown in Fig. 3. Equation (8) is no longer applicable. Second, one sees that the SIE of the X–H bond orbitals (X =B,C) is no longer constant for small R but becomes more negative. Given that there are 8 or 12 electrons in X–H bonds for **2** and **3**, respectively, the SIE of these orbitals dominates the total SIE for small R.

An analysis of the geometry of **2** reveals that the B–H bond length increases and the HBH bond angles decrease for decreasing R: While for $R=3.0$ Å, $r(\mathrm{BH})=1.176$ Å and $\angle(\mathrm{HBH})=157.5°$, at $R=1.8$ Å one finds $r(\mathrm{BH})=1.192$ Å and $\angle(\mathrm{HBH})=147.8°$. This change of the bond length is due to hyperconjugation effects in **2** (Scheme 1): As R decreases, a pseudo-$\pi(\mathrm{BH_2})$ orbital can interact with the empty $2p\pi$ orbital at the other B atom. This leads to a stabilization of the BB bond and the observed elongation of the B–H bonds. As a consequence of hyperconjugation, the B–H bond orbitals

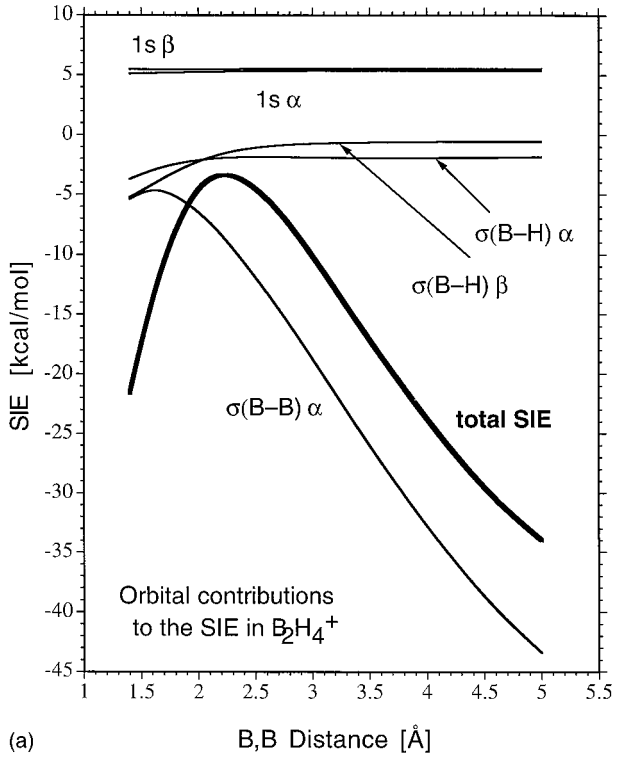

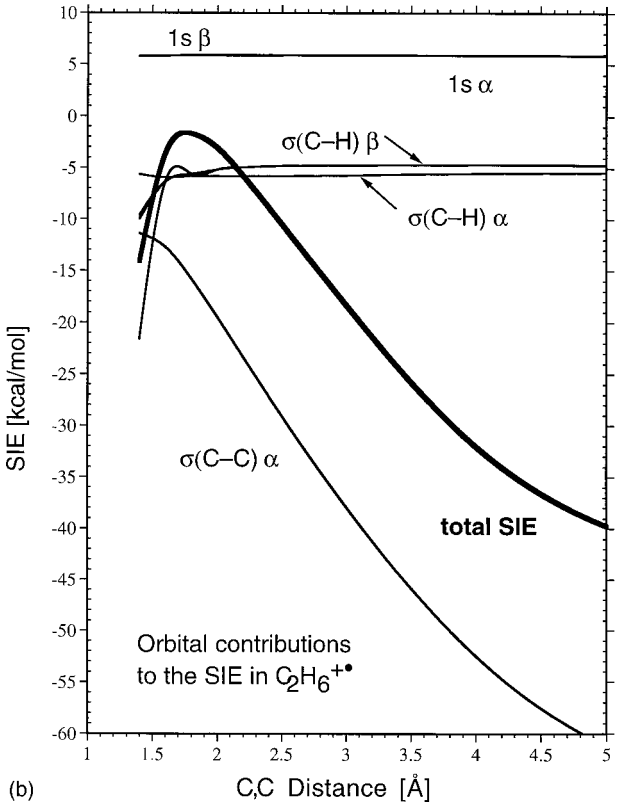

FIG. 4. Orbital contributions to the SIE of (a) $B_2H_4^+$ and (b) $C_2H_6^+$ given as a function of separation distance *R*. Calculations at the P-SIC-BLYP/cc-pVTZ level of theory.

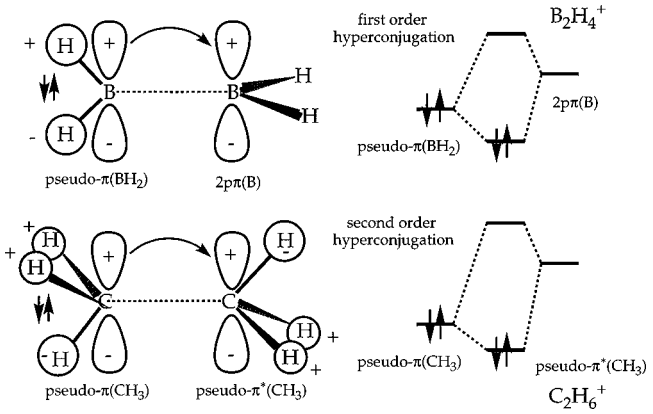

First order hyperconjugation in $B_2H_4^+$ and second order hyperconjugation in $C_2H_6^+$.

become more delocalized, both directly through the hyperconjugation and indirectly through the bond elongation. In addition, the decrease in the HBH bond angle requires a further delocalization of the B–H bond orbitals to maintain orthogonality.

Generally, the SIE for an occupied orbital is more negative the more delocalized this orbital is: The exact self-repulsion of an electron becomes large for a spherically symmetric orbital and small if the orbital is delocalized. The DFT expression for E_X is essentially an integral over ϱ, i.e., it is relatively insensitive to the difference between a ''compact'' (i.e., nearly spherically symmetric) and an extended orbital. Thus, for a given X functional the SIE of an extended orbital is more negative than that of a compact one. The BECKE88 exchange functional[46] is adjusted to noble-gas atoms, i.e., spherical charge distributions. Consequently it yields negative SIEs for extended orbitals.[5]

In **3**, only second order hyperconjugation involving the occupied pseudo-$\pi(CH_3)$ orbitals and the pseudo-$\pi^*(CH_3)$ orbitals can take place. Second-order hyperconjugation is much weaker than first-order hyperconjugation and therefore its effects become only significant at shorter X–X distance. Consequently, the impact of *R* on the geometry of the fragments is smaller: $r(CH)=1.105$ Å and $\angle(HCH)=117.3°$ for $R=1.8$ Å, $r(CH)=1.101$ Å and $\angle(HCH)=119.8°$ for $R=3.0$ Å, and the direct delocalization of the X–H bond orbitals caused by hyperconjugation is weaker than in the case of **2**. This explains that the maximum for the total SIE occurs at a smaller *R* value for **3** than for **2** [Figs. 4(a) and 4(b)]. However, the SIE for **3** becomes strongly *R*-dependent between 1.4 and 1.6 Å. This behavior indicates a change in the orbital occupation: For small *R*, the two degenerate C–C antibonding pseudo-$\pi(CH_3)$ orbitals ($1e_g$-symmetry) are the HOMO's. With increasing distance *R* the $1e_g$-orbitals become less C–C antibonding and are stabilized whereas the $3a_g$ orbital [σ(CC)] is destabilized because of decreasing bonding overlap. For *R* values around the equilibrium bond length and above, the unpaired electron is in the $3a_g$ orbital. For small *R*, in contrast, it is in one of the degenerate $1e_g$ orbitals, which results in a Jahn-Teller distortion[58] and eventually to a change of the SIE contributions of the C–H bond orbitals.

The SIE for the X–H bond orbitals is different for α and β spin. For large *R*, the SIE of the α spin–orbitals is more negative, for small *R*, that of the β spin–orbitals becomes more negative. In the first case, the α X–H bond orbitals have to be orthogonal not only to each other but also to the

X–X bond orbital, which results to an additional delocalization (due to orthogonalization tails) and to a more negative SIE. In the second case, the hyperconjugation effects and the resulting delocalization is more efficient for the β than for the α orbitals because delocalization the latter is limited by interelectronic exchange with the unpaired delocalized α electron of the X–X bond. This explains the difference in the SIEs for small R.

The behavior of the SIE around $R=r_e$ allows us to explain the deviations of the calculated DFT values for r_e and ω_e. If $dE_{cov}^{SIE}/dR>0$ around $R=r_e$, i.e., the SIE leads to an extra stabilization for decreasing R, DFT will underestimate r_e, for $dE_{cov}^{SIE}/dR<0$, i.e., the SIE leads to an extra stabilization for increasing R, r_e will be overestimated. Indeed, we find that DFT gives too large r_e values for **1** and **3** [weak second order hyperconjugation and a dominance of the SIE expressed by Eq. (8)] and too small an r_e value for **2** (strong first order hyperconjugation and a SIE dominated by the BH orbital contributions). P-SIC overestimates the error made in standard DFT calculations whereas for SC-SIC-DFT this overestimation is reduced by orbital relaxations.

The ω_e^a frequencies are directly related to the curvature of the dissociation curve at $R=r_e$. The SIE is a concave function of R at r_e (Fig. 2), hence it makes the curvature of the dissociation curve more negative, which should result in an underestimation of ω_e values. This is confirmed for **1** and **3** but not for **2**. This apparent contradiction can be resolved by considering the bond lengths: For **2**, DFT underestimates the bond lengths and shifts r_e into a region with a stronger curvature of the dissociation curve. The effect of this shift outweights the direct influence of the negative curvature of the SIE term. Conversely, for **1** and **3**, DFT overestimates the bond length, and r_e is shifted into a region with a lower curvature of the dissociation curve, which results in a further underestimation of the ω_e^a values.

B. Dissociation limits and the self-interaction error

In Table III, the relative energies and the electronic stabilities of the covalent and ionic states of **1**, **2**, and **3** for an interaction distance of 10 Å are listed. At the HF level of theory, the ionic state is lower in energy for both **2** and **3** than the covalent one by 18.4 or 15.7 kcal/mol, respectively. Radical cation **1**, on the contrary, does not have an ionic HF state (a BS-UHF solution cannot exist). The ionic ground states are stable, while the covalent state is unstable with respect to a transition of the unpaired electron to either of the two fragments. Adding the LYP correlation functional to the HF exchange gives a slight decrease of the energy splittings (by 3.3 or 2.2 kcal/mol, respectively) to 15.1 and 13.5 kcal/mol (Table III), which does not change the picture qualitatively. However, if the exchange is described partly or completely by a DFT functional the covalent state will become the ground state, and the ionic state is destabilized more strongly the smaller a_{HF} is. The covalent state becomes electronically stable, with the lowest eigenvalue of the Hessian increasing with decreasing a_{HF} (Table III).

The ionic states, in contrast, are less stable electronically and difficult to locate for UDFT. For **1** and **3**, the ionic states are electronically unstable, the smallest λ decreasing with decreasing a_{HF} (Table III). The instability is related to an excitation for the unpaired electron that, depending on the sign of the expansion coefficient, leads to the bonding or the antibonding covalent state of the molecule, respectively. Molecule **2** behaves differently: the ionic states are stable with the smallest λ approximately independent of a_{HF} (values between 0.046 and 0.052; Table III). However, the ionicity of the ionic states of **2** decreases as a_{HF} decreases, and at BLYP this state is nearly covalent. The exceptional behavior of **2** can be related to geometry effects. But before we consider this aspect, the correct dissociation limits of radical cations in general will be discussed. As mentioned in the Introduction, there are misconceptions in the literature, which we want to correct at this point.

1. Experimentally observed dissociation limits and their correct quantum chemical description

In reality, the dissociation of a radical cation with a one-electron bond will always lead to a cationic and a neutral fragment rather than two fragments with charge $+1/2$ each. From this fact it has been concluded (see, e.g., Refs. 33 and 38) that the electronic ground state of a radical cation with a large (but still finite) bond length should be ionic, i.e., break the symmetry of the molecule if there is any. This is, however, not generally correct.

For a dissociating symmetric diatomic radical cation, the ground state is always covalent. It consists of two equivalent fragments with a charge of $+1/2$, which also holds for the first excited state. As the distance of the fragments increases, the excitation energy of the first excited state decreases exponentially. The ground and first excited state can be superimposed to form two equivalent ionic states. These ionic states are, however, no eigenstates but quasistationary states (with a lifetime that grows exponentially as the fragments are drawn apart) and an energy roughly halfway between the energies of the two eigenstates. *The asymmetric dissociation of a symmetric diatomic radical cation can thus not be explained from its electronic ground state alone*. One has to keep in mind that the dissociation is a dynamic process, which cannot be described completely by a zeroth-order Born–Oppenheimer approximation. At some distance R, the unpaired electron will get attached to one of the fragments. Once this has happened it is unlikely that the electron tunnels to the other fragment, so that one is eventually left with a neutral and an ionic fragment. Hence, in reality the dissociation will always take place nonadiabatically and asymmetrically.

The situation is different for polyatomic radical cations provided that geometry relaxation leading to an ionic state is taken into account. In this case, the ionic state will generally have a lower energy than the covalent one due to symmetry-breaking geometry relaxations. If the system under consideration is asymmetric from the beginning as is the case for the MnO^+ and MnO_4^- ions studied by Buijse and co-workers,[18] the ground state and the first excited state of the radical cation are no longer covalent: In the ground state, the unpaired electron is shifted toward the more electronegative fragment, in the excited state to the more electropositive one where this

TABLE III. Energies, stabilities, and ionicities for the covalent and ionic states of radical cations **1**, **2**, and **3**.[a]

Molecule	Method	Geom.[b]	E_{cov}	$E_{ion}-E_{cov}$	λ_{cov}	λ_{ion}	d[c]
1	HF		−0.49982		0.000		
	BH-HLYP		−0.54579	29.64	0.203	−0.089	1.0000
	B3LYP		−0.57790	47.52	0.328	−0.136	1.0000
	BLYP		−0.59440	60.77	0.389	−0.176	1.0000
2	HF	*i*	−51.24008	−18.40	−0.048	0.050	1.0000
		c		−8.13		0.052[d]	1.0000
	HFLYP	*i*	−51.55256	−15.11	−0.038	0.049[d]	1.0000
		c		6.09		−0.038	1.0000
	BH-HLYP	*i*	−51.56842	3.27	0.096[d]	0.047[d]	0.4496
		c		16.02		−0.102	1.0000
	B3LYP	*i*	−51.62313	4.60	0.177[d]	0.046[d]	0.2284
		c		30.00		−0.189	1.0000
	BLYP	*i*	−51.59176	4.83	0.189[d]	0.050[d]	0.1679
		c		37.45		−0.246	1.0000
	SC-SIC-BLYP	*i*	−51.52315	−15.86			1.0000
		c		1.44			1.0000
	MP2	*c*	−51.37692	0.10			1.0000
	CISD	*c*	−51.39840	−2.05			
3	HF	*i*	−78.80041	−15.72	−0.091	0.101	1.0000
		c		−15.50			
	HFLYP	*i*	−79.31621	−13.48	−0.080	0.101	1.0000
		c		−13.41			
	BH-HLYP	*i*	−79.32604	15.17	0.089	−0.097	1.0000
		c		−15.08			
	B3LYP	*i*	−79.40687	33.16	0.169	−0.210	1.0000
		c		33.26			
	BLYP	*i*	−79.36768	45.30	0.165	−0.283	1.0000
		c		45.40			
	SC-SIC-BLYP	*i*	−79.23899	−1.45			1.0000
	SVWN5	*i*	−78.58976	47.00	0.166	−0.293	1.0000
	SC-SIC-SVWN5	*i*	−79.60827	3.94			1.0000
	MP2	*c*	−79.11949	2.60			1.0000
	CISD	*c*	−79.12381	−4.95			

[a]Calculations with Dunning's cc-pVDZ basis set (Ref. 51) for SC-SIC calculations, otherwise with Dunning's cc-pVTZ basis set (Ref. 51). CCSD(T) geometries modified as described in Sec. III were used. The λ values are the lowest eigenvalues of the Hessian matrix. Absolute energies and Hessian eigenvalues in Hartree units, relative energies in kcal/mol.

[b]Geometry at which the ionic state is calculated. *c*, geometry of the covalent state; *i*, geometry of the ionic state.

[c]The ionicity d is given as $d=(q_A-q_B)/(q_A+q_B)$, where q_A and q_B are the charges of the ionic and radicalic parts, respectively.

[d]These states have two (covalent) or one (ionic states) positive Hessian eigenvalues that are smaller than 0.01 Hartree. These eigenvalues are related to $p\sigma\rightarrow p\pi$ excitations for the unpaired electron. The values given in the table are the next-lowest eigenvalues.

effect is more distinct the more the electronegativities of the fragment differ. Obviously, a covalent dissociation limit does no longer exist for the ground state situation.

Both exact wave function theory (WFT) and exact KS-DFT have to yield a covalent ground state for symmetric molecules, as long as geometry relaxation is limited to that of the covalent ground state. For bond lengths around the equilibrium value, the covalent ground state has a high electronic stability and is reproduced qualitatively correctly by approximate computational methods. For long interaction distances, the stability of the covalent state decays to zero, and the covalent and the ionic states become nearly degenerate, consequently there is a continuum of nearly degenerate quasistationary states that are partly ionic. This is shown in Fig. 5. There is no bifurcation from the covalent state into two equivalent ionic states as has been asserted, e.g., in Refs. 33 and 38. The low variance of the total energy with respect to the ionicity implies that even small inconsistencies in practical calculation schemes may influence the picture qualitatively, yielding either a pair of equivalent ionic ground states or a covalent ground state with a nonvanishing stability, and that the predicted ground state depends on the method used.

2. Dissociation limits at the HF level

If all orbitals except that of the unpaired electron were frozen, HF would show the same behavior as exact WFT. However, the UHF orbitals are flexible, which allows to simulate a specific correlation effect occurring in odd-electron bonds: At the fragment where the unpaired electron is to be found, the other electrons are more widely spread into space than at the other fragment. The core orbitals are more diffuse at the fragment that contains the unpaired electron. For the ionic state, this is a simple orbital relaxation effect, which is covered by BS-UHF. Consequently, UHF

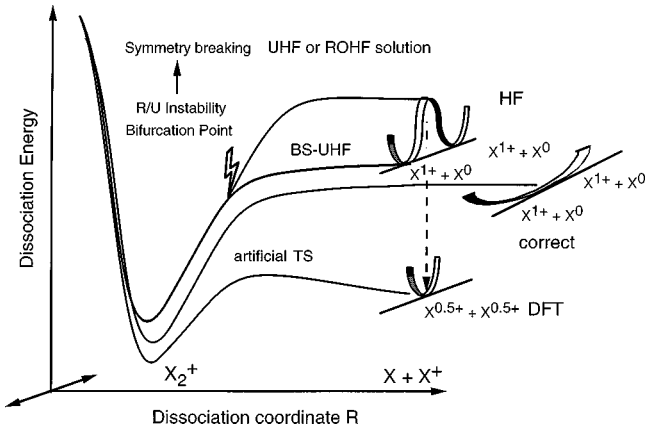

FIG. 5. Schematic representation of the exact, HF, and DFT descriptions of the dissociation of radical cations with one-electron bonds.

will incorrectly favor the ionic over the covalent state [see Ref. 34(b) in this connection]. Consequently, there will be two equivalent ionic ground states and the covalent state will become electronically unstable (see Fig. 5). These effects will be stronger the larger the bond length is, and the ground-state energy as a function of ionicity will bifurcate at some finite bond length (but, to reiterate it, as an artifact of UHF rather than a feature of the real problem).

It should be noted that the energy gain due to the symmetry breaking may be very small. For instance, if Li_2^+ at 20 Å internuclear distance is treated with HF and Pople's 6-311(d) basis set,[59] the energy gain is as small as 0.01 kcal/mol. At 10 Å internuclear distance, the remaining weak covalent binding still outweights the energy gain through symmetry breaking, and the covalent state is stable. This is because for Li_2 there are only weak nondynamic correlation effects between 1s and 2s electrons. For **2** and **3**, in contrast, BS-UHF covers relevant correlations, which is reflected by the energy gain of 8.1 and 15.7 kcal/mol, respectively, relative to the covalent state (at the covalent geometry). The covalent state (as well as the antibonding state) can be regarded as an ''electronic transition state'' that has to be passed when the unpaired electron is moved from one fragment to the other with the wave function kept single-determinantal.

3. Dissociation limits of WFT-based correlated methods

The inclusion of correlations in a WFT method will counteract the inconsistency that occurs at the HF level and the energy curve in dependence of the ionicity will become flatter. It will depend on the method used whether a covalent or an ionic ground state is favored: Methods that tend to exaggerate correlation effects, such as the second-order Møller–Plesset method (MP2) (Ref. 60) will tend to favor the covalent ground state, whereas variational methods such as configuration interaction (CI) can be expected to favor the ionic one. This is corroborated for **2** and **3** where MP2 yields covalent ground states and energy splittings of 0.1 and 2.6 kcal/mol as compared to −18.4 and −15.7 kcal/mol, respectively, for HF (see Table III). CI with single and double excitations (CISD) (Ref. 61) yields ionic ground states with energy splittings of −2.0 and −5.0 kcal/mol. High-level *ab initio* methods based on a HF reference wave function will give nearly identical results for a symmetric and a BS-UHF reference, besides, they will tend to reduce the ionicity of the wave function for a BS-UHF reference as can be seen e.g., in Fig. 1 of Ref. 21 for the case of quadratic CISD (QCISD).[62]

If correlation effects are incorporated by a DFT correlation functional as in HFLYP, the correlation functional will be insensitive to the unbalanced description of the covalent and ionic states. Besides, the DFT correlation functional does not describe the nondynamic correlation effects between the unpaired electron and the paired ones. This is why the inclusion of the LYP correlation functional in HFLYP leaves the predictions from HF essentially unchanged.

4. Dissociation limits at the DFT level of theory

If a BS-UDFT calculation is performed, the ionic states will be stabilized relative to the covalent state in the same way as for BS-UHF. However, this effect will be superimposed and usually outweighed by the influence of the SIE, which was discussed above. Equation (4) shows that for large R, the SIE for the covalent state contains two terms, an R-independent one that favors the covalent state and a term proportional to $1/R$ that favors the ionic state. Usually the first of these terms dominates, which implies that the covalent state is the ground state and has non-vanishing stability for any R (called ''inverse symmetry breaking'' in Ref. 33).

The SIE influences the bonding and the antibonding covalent states in the same way as is shown for the BLYP description of **1** in Fig. 2(a) (the $^2\Sigma_g^+$ and $^2\Sigma_u^+$ state converge to the same limit in the BLYP description), i.e., DFT reflects correctly that the excitation energy decreases exponentially with decreasing R. Consequently, the ionic state is above both the bonding and the antibonding state for large enough R, i.e., it is a fictitious ''electronic transition state'' that has to be passed when the orbital of the unpaired electron is rotated from the bonding to the antibonding state. Just as with the ''electronic transition state'' discussed for the HF solution, this is an artifact of the calculation method with no counterpart in reality. There is no support for the picture given in Ref. 38 that the localized state indicates an avoided crossing between the two covalent states. Such an avoided crossing is not possible for principal reasons. For all R values, the antibonding state is above its bonding counterpart in energy.

5. Dissociation limits predicted by SIC-DFT

For standard DFT, the possible energy gain caused by symmetry breaking is too small to compete with the stabilization of the covalent state by the SIE. In SC-SIC-DFT, the SIE is eliminated. However, the inter-electronic exchange is still described with an approximate DFT functional. The question arises whether this DFT description influences the relative energies of ionic and covalent state. With an estimation similar to that for the SIE shown in Eqs. (5)–(8), one can indeed show that the DFT description of the interelectronic exchange favors the covalent state.

Let ϱ_A^c and ϱ_B^c be the core densities at the two fragments and γ_A^c and γ_B^c the corresponding density matrices; γ_A^v and γ_B^v are the density matrices corresponding to the valence electron densities ϱ_A^v and ϱ_B^v (the unpaired electron in **2** and **3**). The exact interelectronic exchange is given by

$$E_{X,inter}^{exact}\int d^3r_1\int d^3r_2\,\gamma_A^v(\mathbf{r}_1,\mathbf{r}_2)\,\gamma_A^c(\mathbf{r}_1,\mathbf{r}_2)\,\frac{1}{r_{12}}-E_{X,intra,A}^{exact} \tag{9}$$

both for the ionic and the covalent state. Here, $E_{X,intra,A}^{exact}$ is the intraelectronic exchange for the core electrons in fragment A, which is independent of the position of the valence electron. The LDA interelectronic exchange energies for the covalent and the ionic state are

$$E_{X,inter,ion}^{DFT}=-C_X\int d^3r\{[\varrho_A^v(\mathbf{r})+\varrho_A^c(\mathbf{r})]^{4/3}-\varrho_A^v(\mathbf{r})^{4/3}+\varrho_B^c(\mathbf{r})^{4/3}\}-E_{X,intra,A+B}^{DFT}, \tag{10a}$$

$$E_{X,inter,cov}^{DFT}=-C_X\int d^3r\left\{\left[\frac{1}{2}\varrho_A^v(\mathbf{r})+\varrho_A^c(\mathbf{r})\right]^{4/3}-\frac{1}{2}\varrho_A^v(\mathbf{r})^{4/3}+\left[\frac{1}{2}\varrho_B^v(\mathbf{r})+\varrho_B^c(\mathbf{r})\right]^{4/3}-\frac{1}{2}\varrho_B^v(\mathbf{r})^{4/3}\right\}-E_{X,intra,A+B}^{DFT}, \tag{10b}$$

where $C_X=(3/2)(3/4\pi)^{1/3}$. $E_{X,intra,A+B}^{DFT}$ is the intraelectronic exchange for all core electrons in fragments A and B, which does not depend on the position of the bonding valence electron. Keeping in mind the symmetry between fragments A and B, this leads to

$$E_{X,inter,ion}^{DFT}-E_{X,inter,cov}^{DFT}=-C_X\int d^3r\left[\xi(\varrho_A^v(\mathbf{r});\varrho_A^c(\mathbf{r}))+\xi(0;\varrho_A^c(\mathbf{r}))-2\xi\left(\frac{1}{2}\varrho_A^v(\mathbf{r});\varrho_A^c(\mathbf{r})\right)\right], \tag{11a}$$

where the function ξ is defined as

$$\xi(x;y)=(x+y)^{4/3}-y^{4/3}. \tag{11b}$$

For all positive values of x, y, $\partial^2\xi/\partial x^2<0$ for all x, i.e., ξ is a concave function of x, and it holds

$$\xi(x;y)+\xi(0;y)-2\xi(x/2;y)<0 \quad \text{for all } x,y>0. \tag{12}$$

Hence, the integrand in Eq. (11a) is always negative, and consequently $E_{X,inter}^{DFT}$ is smaller in magnitude for the ionic than for the covalent state. As a correct description should give the same interelectronic exchange energy for ionic and covalent state, this result shows that LDA overstabilizes the covalent state relative to the ionic one. As the LDA part is the main contribution to a GGA functional, the same should hold true for the GGA description. It is interesting to note that the energy difference brought in by the DFT description of the interelectronic exchange is independent of R, i.e., does not give rise to an artificial transition state in the dissociation curve or a Coulomb repulsion between the fragments.

For SC-SIC-DFT the relative energy of covalent and ionic state are governed by two opposing effects, which may be of the same order of magnitude. The BS-SC-SIC description favors the ionic dissociation limit whereas at the same time the symmetry-adapted SC-SIC-DFT solution stabilizes the covalent dissociation limit. Accordingly, the energy splitting between covalent and ionic states becomes relatively small for SC-SIC-DFT (<1.5 kcal/mol for both **2** and **3** if BLYP is used, Table III). One can no longer predict the energy ordering of the two states because there is no clear rationale to predict which of the two factors is larger in magnitude for a given radical cation. In this sense, SC-SIC-DFT allows, thanks to a fortuitous compensation of errors, a more balanced description of the covalent and ionic state of one-electron-bonded molecules than either HF or DFT. This, however, does not contradict the conclusion given above that SIC-DFT does not provide a real improvement relative to either HF or standard DFT.

6. Influence of geometry relaxation on the dissociation limit

It remains to discuss the influence of geometry relaxation on the dissociation limits. Figure 1 shows that for the ionic state of **2** the fragments have clearly different geometries in distinction to the case of **3**. These differences in geometry can be explained with the Walsh counting rules:[58] $\mathbf{4}^+$ has $D_{\infty h}$ symmetry and the electron configuration $(1\sigma_g)^2(2\sigma_g)^2(2\sigma_u)^2$. The $2\sigma_u$ electrons are B–H bonding and H–H antibonding, thus they favor a linear geometry for $\mathbf{4}^+$. In $\mathbf{4}^{\bullet}$, the additional electron is in a $1\pi_u$ orbital. The linear form of the molecule becomes unstable due to a second order Jahn-Teller effect and the radical adopts a bent form with a HBH bond angle of 128.5°. These geometry differences contribute essentially to the energy ordering for **2**.

For the purpose of separating electronic and geometry effects we calculated the ionic state of **2** both at its optimized geometry and at the geometry of the covalent state. The ionic states calculated at the geometry of the covalent state are, for HFLYP through BLYP, 20–33 kcal/mol higher in energy than the same states calculated at their equilibrium geometry (''ionic geometry''). For **3**, in contrast, the energy difference of the ionic states at the covalent and ionic geometries is at most 0.22 kcal/mol (see Table III), i.e., small compared to the energy differences between the two states. As mentioned before for SC-SIC-BLYP, the covalent and ionic states will be close to each other in energy if both states are calculated at the covalent geometry; the absolute value of the energy splitting is about 1.5 kcal/mol for both **2** and **3**. The energy ordering cannot be predicted and may also depend on the functional chosen as the SC-SIC-SVWN5 results for **3** show.

Clearly, when discussing ionic and covalent dissociation one has to consider the geometry relaxation effects in the fragments generated because these can favor an asymmetric (symmetry broken) ionic dissociation. Since the geometry relaxation effects are strong in the case of **2** ionic dissociation approaches the covalent dissociation predicted by all DFT methods closely whereas in the case of **3** it is 45 kcal/

mol (BLYP, Table III) above the preferred covalent dissociation.

7. The SIE of the fragments

So far, only the SIE of the dissociating supermolecule has been discussed. The SIE of the fragments is relatively small and compensates partly the SIE for the core electrons in the supermolecule. For $\mathbf{5}^{\bullet}$, however, SIC-DFT leads to an inconsistency between supermolecule and fragment: Radical $\mathbf{5}^{\bullet}$ is planar, which is described correctly both by wavefunction and standard DFT methods. The SIC-DFT ground state form of $\mathbf{5}^{\bullet}$, however, is pyramidal. P-SIC-BLYP/cc-pVDZ yields an energy 4.9 kcal/mol below that of the planar form at a pyramidalization angle of 32.2° (Fig. 1). This artifact can be comprehended based on the different orbital localization patterns for the two geometries: Whereas for planar $\mathbf{5}^{\bullet}$, there are three sp^2(C–H) orbitals and one (unpaired) $p\pi$ orbital, the unpaired orbital in the pyramidal form gets partial *s* character and four sp^3 hybrid orbitals are formed. Because of the rehybridization, the SIE per C–H bond orbital increases from $|-3.8|$ to $|-4.6|$ kcal/mol, whilst the SIE of the unpaired electron decreases from $|-23.8|$ to $|-14.5|$ kcal/mol. This is due to a lengthening of the C–H bonds (more expanded bond orbitals lead to a larger magnitude of the SIE) and the change from a $p\pi$ to a sp^3 orbital (with increasing *s*-character the orbital becomes more compact and the magnitude of the SIE is reduced). Together with small changes in the SIE of the remaining orbitals, the total SIE changes from $|-32.5|$ (planar) to $|-26.4$ kcal/mol (pyramidal), i.e., the planar form is stabilized by 6.1 kcal/mol relative to the pyramidal form at the BLYP level of theory. Accordingly, the planar form becomes destabilized at P-SIC-BLYP leading to a barrier to planarity of 4.9 kcal/mol where changes in the nuclear repulsion energy play also a role. For SC-SIC-BLYP/cc-pVDZ//P-SIC-BLYP/cc-pVDZ, the stabilization energy of the pyramidal form is 5.6 kcal/mol.

Due to the additional stabilization of $\mathbf{5}^{\bullet}$, the D_e value for **3** reduces to 49.0 kcal/mol (P-SIC-BLYP) and 50.9 kcal/mol (SC-SIC-BLYP), respectively. The corrected value for SC-SIC is closer to the CCSD(T) reference value (52.5 kcal/mol, Table I) than the original one. Still, the inconsistency for fragment $\mathbf{5}^{\bullet}$ shows that the lack of unitary invariance in SIC-DFT may give rise to an unbalanced description e.g., of reactant and reaction products. This may be particularly problematic when orbitals undergo a major rearrangement, as e.g., in transition states, i.e., just in those cases where the application of SIC-DFT is most interesting otherwise.

V. CONCLUSIONS AND OUTLOOK

The proper description of dissociating radical cations with one-electron bonds is subtle for two reasons: (i) As the fragments are removed from each other, the energy difference between the covalent and the ionic state of the molecule decreases exponentially, and even a relative small inconsistency in the calculational method used can influence the results qualitatively. (ii) In the covalent state, the valence electron, and consequently its exchange hole, is distributed over a large region in space. Several computational methods, in particular standard KS-DFT fail to describe this extended exchange hole correctly.

(1) In the correct description, the multitude of covalent, partially ionic, and ionic states (charge q increasing from 0 to 1, see Fig. 5) must be quasidegenerate for large separation distance R. A computational scheme that favors either the covalent or the ionic ground state is erroneous where the magnitude of the error can be directly derived from the energy difference between covalent and ionic states. A quite common misconception in the literature is that, beyond a certain R, the ground state of the system should always be ionic and, consequently, it is an advantage of a given computational method to predict the ionic ground state (see e.g., Refs. 33 and 38).

(2) It is possible that by geometry relaxations in the fragments the ground state will become ionic. For **1**, this possibility is excluded and for **3** the effect is small. If geometry relaxation becomes strong because one of the fragments can undergo a second-order Jahn-Teller distortion, as found in the case of **2**, the correct description will always favor the ionic state. However, as long as both states are considered at the same geometry an accurate method has to predict a covalent ground state with a stability that decays to zero rapidly as the interaction distance increases. Our calculations show that this is indeed the case for CCSD(T).

(3) The fact that UHF predicts even for a symmetric geometry an ionic ground state indicates that the treatment of electron correlation in the ionic and the covalent state is not balanced, similar as it is the case with the RHF and the UHF descriptions of a bond breaking.

(4a) KS-DFT with the approximate XC functionals in use suffers from a large SIE caused by the exchange functional. Investigation of the exchange hole shows that for larger R the SIE is due to the unpaired electron, for which DFT exchange simulates long-range electron correlation effects with a second electron in the same orbital that of course does not exist. This leads to an artificial stabilization increasing with distance R to a limit value that is equal to the self-exchange of one electron. For a bonded electron pair, the SIE can compensate lacking nondynamic Coulomb correlation between two electrons, but as soon as the electron number in the bond decreases the effect mimicked by the SIE becomes superfluous and leads to a nonphysical description. The maximum error will be found for the one-electron bond.

(4b) The SIE exchange hole is related to the SIE energy via the electron density. In the covalent state, the SIE is decreased for R values larger than the r_e by an artificial self-repulsion potential between the two halves of the electron, which can be approximated by the expression $1/4R$. With increasing R the artificial Coulomb repulsion potential decays to zero thus leading to the self-exchange of one electron and the maximum stabilization of the covalent state.

(5) It is shown for the first time that DFT interelectronic exchange leads to an additional stabilization of the cova-

lent state relative to the ionic states of the dissociating radical cations. This error is still present in the SIC-DFT description of the radical cations.

(6) P-SIE and SC-SIE differ considerably where these differences become larger for increasing *R*. P-SIC exaggerates the energy correction whereas SC-SIC reduces the effects of P-SIC via orbital relaxation. In general, the SC-SIC-DFT orbitals are more contracted than the DFT orbitals because the SIE leads to an expansion of the orbitals. It is important to note that SIC has to be treated self-consistently. Perturbational SICs indeed correct the artificial Coulomb repulsion and reduce the energy deviation between supermolecule and fragments but do not yield the correct energy of the molecule at large bond lengths.

(7) The SIE given as a function of *R* has an inflection point because SIE(*R*) is concave close to the equilibrium X–X bond distance, however convex for larger *R*. The maximum of SIE(*R*) (i.e., a SIE close to zero) found at a critical *R* value typical of the radical cation investigated is influenced by a maximum compensation between Coulomb self-repulsion and self-exchange. For *R* smaller than the critical *R* the SIE increases again in magnitude. It was shown that this is caused by the SIE contributions of the XH bond orbitals which become more delocalized by first order (**2**) or second order hyperconjugation (**3**). Since the former effect is much stronger than the latter effect, the maximum of SIE(*R*) and the increase in the magnitude of the SIE occurs at larger *R* for **2** than for **3**. Accordingly, the equilibrium X–X distance of the latter radical cation is affected by the SIE of the unpaired α-electron (DFT yields too long a X–X bond) whereas for **2** the SIE is affected of the B–H electrons (DFT yields too short a X–X distance).

(8) The SIE of the excited (antibonding) covalent state in the case of **1** (and probably also in the cases of **2** and **3**) is of the same magnitude as in the ground state. Therefore, the excitation energies from ground to excited state are correctly described. Nevertheless the mixing between ground and excited state does not necessarily lead to a broken symmetry solution of ionic nature as at the HF level of theory. This is a result of the stabilization of the covalent states by both SIE and interelectronic exchange.

(9) In those cases where standard DFT leads to an ionic state for large *R* it is described correctly, in particular if a modern gradient-corrected functional is used. Using the energy difference between the higher lying ionic state and the covalent state as an appropriate criterion for the accuracy of the method used, DFT yields large differences, which decrease when more exact exchange is mixed to DFT exchange.

(10) SIC-DFT seems to lead to an improved description of radical cations with one-electron bonds as it predicts (a) qualitatively correct dissociation curves and (b) a dissociation limit, for which covalent and ionic states are separated by just a few kcal/mol. We have shown in this work that the latter point is the result of a fortuitous cancellation of the error caused by interelectronic DFT exchange (stabilizing the covalent state) and the extra correlation effects included by BS-SIC (stabilizing the ionic state). Otherwise, SIC-DFT fails to describe the equilibrium properties of the radical cations correctly.

(11) The fragment geometry of $CH_3^{\bullet}$ is wrongly described by SIC-DFT predicting a pyramidal rather than a planar form. Utilizing the calculated orbital SIEs, we could explain this as a result of an unbalanced DFT description of planar and pyramidal form, which becomes obvious when the SIE is corrected. This leads to an improvement of the dissociation energy of **3**, reveals however another shortcoming of SIC-DFT, which makes it use rather problematic.

The conclusions drawn for the radical cations are directly relevant for DFT descriptions of transition states and charge transfer complexes involving an odd number of electrons. In these cases, standard DFT will give a qualitatively incorrect picture if the unpaired electron is distributed over two ore more atomic centers.[63] Using a hybrid exchange functional reduces the error, but even for BH-HLYP calculated energies may be wrong by several 10 kcal/mol. There are a number of efforts to introduce functionals that correct for the SIE. SC-SIC-DFT suggested by Perdew and Zunger and programmed in this work is computationally demanding and abandons thus one of the main advantages of standard DFT. A routine investigation of systems with delocalized unpaired electrons requires thus methods that correct the SIE while avoiding the computational drawbacks of Perdew–Zunger SC-SIC-DFT. The development of such methods is a challenging task. One way may be to refine the available approximate XC functionals. As the local density, its gradient and possibly Laplacian do not contain information on the features of the system at large distances of the reference point; this will require functionals that essentially differ from the currently available ones. In view of the results obtained in this work, the solution of the SIE problem cannot be its elimination without changing the correlation functional. This is because

(a) important long-range correlation effects are deleted also in those cases where they are needed;
(b) the interelectronic exchange error of DFT becomes a non-negligible problem.

It is a better solution to use directly exact exchange and to describe the long-range correlation effects via the correlation functional. A trivial way to accomplish this is to introduce standard DFT exchange functionals into the correlation functional. Perdew and Schmidt[63] have suggested such a functional, which may be most promising to correctly describe both delocalized exchange holes and long-range correlation without giving up the simplicity of standard DFT.

ACKNOWLEDGMENTS

We thank Dr. Victor Polo for carrying out preliminary calculations for this project. This work was supported by the Swedish Research Council (Vetenskapsrådet). An allotment of computer time at the National Supercomputer Center (NSC) at Linköping is gratefully acknowledged.

[1] D. Cremer, Mol. Phys. **99**, 1899 (2001).
[2] V. Polo, E. Kraka, and D. Cremer, Mol. Phys. **100**, 1771 (2002).
[3] V. Polo, E. Kraka, and D. Cremer, Theor. Chem. Acc. **107**, 291 (2002).
[4] V. Polo, J. Gräfenstein, E. Kraka, and D. Cremer, Chem. Phys. Lett. **352**, 469 (2002).
[5] V. Polo, J. Gräfenstein, E. Kraka, and D. Cremer, Theor. Chem. Acc. **107**, 291 (2002).
[6] D. Cremer, M. Filatov, V. Polo, E. Kraka, and S. Shaik, Int. J. Mol. Sci. **3**, 604 (2002).
[7] M. Filatov and D. Cremer, J. Chem. Phys. **5**, 2320 (2003).
[8] P. Hohenberg and W. Kohn, Phys. Rev. **136**, B864 (1964).
[9] W. Kohn and L. J. Sham, Phys. Rev. **140**, A1133 (1965).
[10] (a) J. P. Perdew, *Local Density Approximations in Quantum Chemistry and Solid State Physics*, edited by J. Avery and J. P. Dahl (Plenum, New York, 1984); (b) J. P. Perdew and M. Ernzerhof, *Electronic Density Functional Theory: Recent Progress and New Directions*, edited by J. F. Dobson, G. Vignale, and M. P. Das (Plenum, New York, 1998), p. 31.
[11] J. P. Perdew and A. Zunger, Phys. Rev. B **23**, 5048 (1981).
[12] L. Noodleman, D. Post, and E. J. Baerends, Chem. Phys. **64**, 159 (1982).
[13] (a) J. G. Harrison, R. A. Heaton, and C. C. Lin, J. Phys. B **16**, 2079 (1983); (b) M. R. Pederson, R. A. Heaton, and C. C. Lin, J. Chem. Phys. **80**, 1972 (1984); (c) **82**, 2688 (1985).
[14] (a) J. B. Krieger and Y. Li, Phys. Rev. A **39**, 6052 (1989); (b) Y. Li and J. B. Krieger, *ibid.* **41**, 1701 (1990); (c) J. Chen, J. B. Krieger, and Y. Li, *ibid.* **54**, 3939 (1996).
[15] (a) Y. Guo and M. A. Whitehead, J. Comput. Chem. **12**, 803 (1991); (b) M. A. Whitehead and S. Suba, *Recent Advances in Computational Chemistry*, edited by D. P. Chong (World Scientific, Singapore, 1995), Vol. 1, Part I, p. 53.
[16] P. M. W. Gill, B. G. Johnson, C. A. Gonzales, and J. A. Pople, Chem. Phys. Lett. **221**, 100 (1994).
[17] S. Goedecker and C. J. Umrigar, Phys. Rev. A **55**, 1765 (1977).
[18] M. A. Buijse and E. J. Baerends, Theor. Chim. Acta **79**, 389 (1991); J. Chem. Phys. **93**, 4129 (1990).
[19] (a) X. M. Tong and S. I. Chu, Phys. Rev. A **55**, 3406 (1997); (b) **57**, 855 (1998); (c) T. F. Jiang, X. M. Tong, and S. I. Chu, Phys. Rev. B **63**, 45317 (2001).
[20] (a) R. K. Nesbet, Phys. Rev. A **56**, 2665 (1997); (b) Int. J. Quantum Chem. **85**, 405 (2001).
[21] (a) G. I. Csonka, N. A. Nguyen, and I. Kolossvary, J. Comput. Chem. **18**, 1534 (1997); (b) G. I. Csonka and B. G. Johnson, Theor. Chem. Acc. **99**, 158 (1998).
[22] K. Burke, J. P. Perdew, and M. Ernzerhof, J. Chem. Phys. **109**, 3760 (1998).
[23] O. V. Gritsenko, B. Ensing, P. R. T. Schipper, and E. J. Baerends, J. Phys. Chem. A **104**, 8558 (2000).
[24] (a) J. Garza, J. A. Nichols, and D. A. Dixon, J. Chem. Phys. **112**, 7880 (2000); (b) **113**, 6029 (2000); (c) J. Garza, R. Vargas, J. A. Nichols, and D. A. Dixon, *ibid.* **114**, 639 (2001).
[25] F. D. Sala and A. Görling, J. Chem. Phys. **115**, 5718 (2001).
[26] (a) S. Patchkovskii, J. Autschbach, and T. Ziegler, J. Chem. Phys. **115**, 26 (2001); (b) S. Patchkovskii and T. Ziegler, *ibid.* **116**, 7806 (2002); (c) S. Patchkovskii and T. Ziegler, J. Phys. Chem. A **106**, 1088 (2002).
[27] S. Kümmel and J. P. Perdew, Mol. Phys. **101**, 1363 (2003).
[28] N. C. Handy and A. J. Cohen, Mol. Phys. **99**, 403 (2001).
[29] E. Fermi and E. Amaldi, Accad. Ital. Rome **6**, 119 (1934).
[30] J. C. Slater, *Quantum Theory of Molecules and Solids (The Self-Consistent Field for Molecules and Solids)* (McGraw–Hill, New York, 1974), Vol. 4.
[31] R. Merkle, A. Savin, and H. Preuss, J. Chem. Phys. **97**, 9216 (1992).
[32] E. Ruiz, D. R. Salahub, and A. Vela, J. Chem. Phys. **100**, 12265 (1996).
[33] T. Bally and G. N. Sastry, J. Phys. Chem. A **101**, 7923 (1997).
[34] (a) B. Braïda and P. C. Hiberty, J. Phys. Chem. A **102**, 7872 (1998); (b) B. Braïda, D. Lauvergnat, and P. C. Hiberty, J. Chem. Phys. **115**, 90 (2001).
[35] (a) Y. Zhang and W. Yang, J. Chem. Phys. **109**, 2604 (1998); (b) Y. Zhang and W. Yang, Theor. Chem. Acc. **103**, 346 (2001).
[36] M. Sodupe, J. Bertran, L. Rodríguez-Santiago, and E. J. Baerends, J. Phys. Chem. **103**, 166 (1999).
[37] Y. Xie, H. F. Schaefer III, X. Y. Fu, and R. Z. Liu, J. Chem. Phys. **111**, 2532 (1999).
[38] H. Chermette, I. Ciofini, F. Mariotti, and C. Daul, J. Chem. Phys. **114**, 1447 (2001).
[39] M. Grüning, O. V. Gritsenko, S. J. A. van Gisbergen, and E. J. Baerends, J. Phys. Chem. **105**, 9211 (2001).
[40] J. Jaramillo and G. E. Scuseria, J. Chem. Phys. **118**, 1068 (2003).
[41] E. Kraka, J. Gräfenstein, M. Filatov, J. Gauss, A. Wu, V. Polo, Y. He, F. Reichel, L. Olsson, Z. Konkoli, Z. He, and D. Cremer, COLOGNE 2003 (Göteborg University, Göteborg, 2003).
[42] J. M. Foster and S. F. Boys, Rev. Mod. Phys. **32**, 300 (1960).
[43] R. Seeger and J. A. Pople, J. Chem. Phys. **65**, 265 (1976).
[44] M. R. Hestenes and E. Stiefel, J. Res. Natl. Bur. Stand. **49**, 409 (1952).
[45] C. Lee, W. Yang, and R. G. Parr, Phys. Rev. B **37**, 785 (1988).
[46] A. D. Becke, Phys. Rev. A **38**, 3098 (1988).
[47] A. D. Becke, J. Chem. Phys. **98**, 5648 (1993).
[48] A. D. Becke, J. Chem. Phys. **98**, 1372 (1993).
[49] S. H. Vosko, L. Wilk, and M. Nusair, Can. J. Phys. **58**, 1200 (1980).
[50] K. Raghavachari, G. W. Trucks, J. A. Pople, and M. Head-Gordon, Chem. Phys. Lett. **157**, 479 (1989).
[51] T. H. Dunning, Jr., J. Chem. Phys. **90**, 1007 (1989).
[52] (a) Z. Konkoli and D. Cremer, Int. J. Quantum Chem. **67**, 1 (1998); (b) **67**, 29 (1998); (c) D. Cremer, J. A. Larsson, and E. Kraka, in *Theoretical and Computational Chemistry*, edited by C. Párkányi (Elsevier, Amsterdam, 1998), Vol. 5, p. 259.
[53] J. C. Slater, Phys. Rev. **81**, 385 (1951).
[54] R. Seeger and J. A. Pople, J. Chem. Phys. **66**, 3045 (1977).
[55] R. Bauernschmitt and R. Ahlrichs, Chem. Phys. **104**, 9047 (1996).
[56] J. F. Stanton, J. Gauss, J. D. Watts, W. J. Lauderdale, and R. J. Bartlett, ACES II, Quantum Theory Project, University of Florida, 1992; see also, J. F. Stanton, J. D. Watts, W. J. Lauderdale, and R. J. Bartlett, Int. J. Quantum Chem., Quantum Chem. Symp. **26**, 879 (1992).
[57] M. J. Frisch, G. W. Trucks, H. B. Schlegel *et al.*, GAUSSIAN 98, Revision A.9 (Gaussian, Inc., Pittsburgh, Pennsylvania, 1998).
[58] See, e.g., T. A. Albright, J. K. Burdett, and M. H. Whangbo, *Orbital interactions in Chemistry* (Wiley–Interscience, New York, 1985).
[59] R. Krishnan, M. Frisch, and J. A. Pople, Chem. Phys. **72**, 4244 (1980).
[60] C. Møller and M. S. Plesset, Phys. Rev. **46**, 618 (1934). For a recent review, see D. Cremer, in *Encyclopedia of Computational Chemistry*, edited by P. V. R. Schleyer, N. L. Allinger, T. Clark, J. Gasteiger, P. A. Kollman, H. F. Schaefer III, and P. R. Schreiner (Wiley, Chichester, 1998), Vol. 3, p. 1706.
[61] J. A. Pople, J. S. Binkley, and R. Seeger, Int. J. Quantum Chem., Symp. **10**, 1 (1976).
[62] J. A. Pople, M. Head-Gordon, and K. Raghavachari, J. Chem. Phys. **87**, 5968 (1987).
[63] J. P. Perdew and K. Schmidt, *Density Functional Theory and its Application to Materials*, edited by V. E. Van Doren, K. Van Alsenoy, and P. Geelings (American Institute of Physics, New York, 2001).